

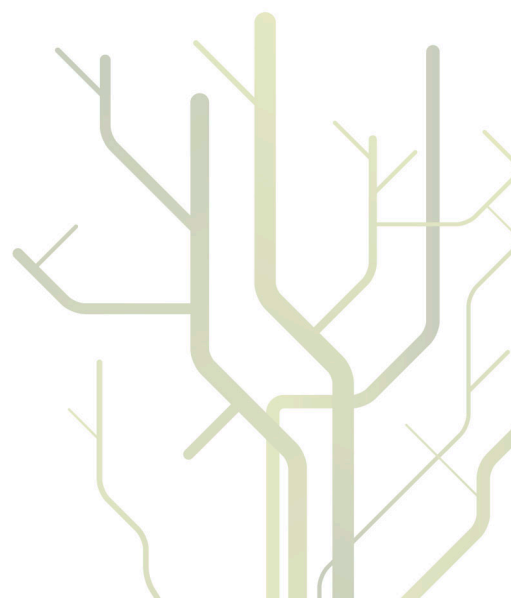
Understanding and predicting one- and two-photon absorption properties of molecular complexes



Arnfinn Hykkerud Steindal

A dissertation for the degree of
Philosophiae Doctor

November 2012



Abstract

This thesis presents the development of theoretical models for the calculations of one- and two-photon absorption, and computational studies on solvated systems and biomolecules. The photon-absorbing chromophore is described by density functional theory, while the effects of the surroundings are taken into account by means of polarizable embedding models. The theory and implementation of a three-layered fully polarizable method is presented in this thesis. In this method, the short-range electrostatic potential due to the solvent is treated by a polarizable molecular mechanics force field, while the long-range effects are described by a dielectric continuum. This QM/MM/PCM implementation was tested on three organic molecules solvated in water and shown to converge faster with respect to system size compared to calculations using quantum mechanics/molecular mechanics (QM/MM) only. Further, the parallelization of the QM/MM module in the Dalton program is described, making it possible to do calculations on large molecular systems with the use of modern supercomputers. This implementation was used to calculate the one- and two-photon absorption properties in fluorescent proteins, demonstrating the importance of describing the protein surrounding the chromophore by a polarizable embedding.

Acknowledgements

I wish to thank, first and foremost, my supervisor Luca for his support and guidance, and for always trying to answer my not-so-well-phrased questions.

My thanks go also to my two co-supervisors: Kenneth, his excellent knowledge about the Dalton-beast has been extremely helpful; and Bjørn Olav for introducing me to the computational-chemistry-world outside Dalton and quantum mechanics.

I would also like to thank Jacob and Jógvan for inspiring collaboration, helpful discussions, technical assistance, and for making my stay in Odense very pleasant. This thesis would not have been possible without you.

All my present and former colleagues at CTCC are thanked for creating a friendly, inspiring environment. Especially I would like to thank all my colleagues I have shared office with during all these years, and annoyed with all my questions, in chronological order: Jonas, Stig Rune, Ville, Chris, Jógvan and Maarten. I also would like to thank the HPC group at the UiT for helping me out with my (often self-made) technical problems, Stig for helping me out with all the paper work (especially related to my often complicated parental leave plans), and Jonas and Radovan for being my unix-gurus.

In addition I would like to share the credit of my work with my co-authors Kęstutis, Maarten, Nanna and Hans Jørgen. You made my life much easier.

Thanks to all my friends, and family for being so supportive and at least pretending to understand what my PhD was all about, and Gunn for taking care of my kids so I was able to finish it.

Finally, I would like to thank my wife Anne Linn for being so patient and encouraging, and my three wonderful kids Ingeborg, Anna and Hilmar, for making me understand that there are more important things in life than work. This thesis is dedicated to them.

Tromsø, November 2012

A handwritten signature in blue ink, appearing to read "Arnfinn Hykkerud Steindal". The signature is written in a cursive, somewhat stylized script.

Arnfinn Hykkerud Steindal

Contents

Abstract	I
Acknowledgements	III
List of Papers	VII
Preface	1
1 Ground-state quantum mechanics	3
1.1 Wavefunctions and Schrödinger equations	3
1.2 Hartree-Fock	7
1.3 Density Functional Theory	9
1.3.1 The exchange-correlation functionals	12
2 Polarizable embedding	15
2.1 IEF-PCM	18
2.2 QM/MM	21
3 Molecular Electronic Properties	27
3.1 Time-dependent DFT	27
3.2 Response theory	28
3.2.1 KS-DFT response functions	30
3.3 PE contributions to the response functions	35
3.3.1 QM/MM response contributions	35
3.3.2 PCM response contributions	36

4	Summary of the papers	39
4.1	The three-layered QM/MM/PCM model	39
4.2	Parallelization of the QM/MM module	41
4.3	Polarizable embedding on fluorescent proteins	42

List of Papers

This thesis is based on the following scientific papers

- I **A. H. Steindal**, K. Ruud, L. Frediani, K. Aidas and J. Kongsted: “Excitation energies in solution: the fully polarizable QM/MM/PCM method”, *J. Phys. Chem.*, 2011, **115**, 3027-3037
- II **A. H. Steindal**, J. M. H. Olsen, L. Frediani, J. Kongsted and K. Ruud: “Parallelization of the polarizable embedding scheme for higher-order response functions”, *Mol. Phys.*, 2012, **110**, 2579-2586
- III **A. H. Steindal**, J. M. H. Olsen, K. Ruud, L. Frediani and J. Kongsted: “A combined quantum mechanics and molecular mechanics study of the one- and two-photon absorption in the green fluorescent protein”, *Phys. Chem. Chem. Phys.*, 2012, **14**, 5440-5451
- IV M. T. P. Beerepoot, **A. H. Steindal**, J. M. H. Olsen, K. Ruud, L. Frediani, B. O. Brandsdal and J. Kongsted: “A polarizable embedding DFT study of one-photon absorption in fluorescent proteins”, Manuscript
- V N. H. List, J. M. H. Olsen, H. J. Aa. Jensen, **A. H. Steindal** and J. Kongsted: “Molecular-level insight into the spectral tuning mechanism of the DsRed chromophore”, *J. Phys. Chem. Lett.*, 2012, **3**, 3513-3521

Other (related and unrelated) scientific papers not included in this thesis

- Z. Rinkevicius, N. A. Murugan, J. Kongsted, B. Frecuş, **A. H. Steindal** and H. Ågren, *J. Chem. Theory Comput.*, 2011, **7**, 3261-3271.
- Z. Rinkevicius, N. A. Murugan, J. Kongsted, K. Aidas, **A. H. Steindal** and H. Ågren, *J. Phys. Chem. B*, 2011, **115**, 4350-4358.
- T. T. Thu Tam, A. Juzeniene, **A. H. Steindal**, Vladimir Iani and J. Moan, *J. Photochem. Photobiol. B: Biol.*, 2009, **94**, 201-204.
- A. Juzeniene, R. Setlow, A. Porojnicu, **A. H. Steindal** and J. Moan, *J. Photochem. Photobiol. B: Biol.*, 2009, **96**, 93-100.
- **A. H. Steindal**, T. T. Thu Tam, X. Y. Lu, A. Juzeniene and J. Moan, *Photochem. Photobiol. Sci.*, 2008, **7**, 814-818.
- **A. H. Steindal**, A. C. Porojnicu and J. Moan, *Med. Hypotheses*, 2007, **69**, 182-185.
- **A. H. Steindal**, A. Juzeniene, A. Johnsson and J. Moan, *Photochem. Photobiol.*, 2006, **82**, 1651-1655.
- P. Vorobey, **A. E. Steindal**, M. K. Off, A. Vorobey, and J. Moan, *Photochem. Photobiol.*, 2006, **82**, 817-822.
- L. W. Ma, **A. E. Steindal**, A. Juzeniene, V. Iani and J. Moan, *Photochem. Photobiol. Sci.*, 2006, **5**, 755-759.
- M. K. Off, **A. E. Steindal**, A. C. Porojnicu, A. Juzeniene, A. Vorobey, A. Johnsson, and J. Moan, *J. Photochem. Photobiol. B: Biol.*, 2005, **80**, 47-55.

Preface

In recent years, computational modelling has become an indispensable tool for many researcher in the fields of physics and chemistry. An important goal of such *in silico* modelling is not only to reproduce but also to predict the outcome of experiments. In computational chemistry we are interested in reproducing and predicting experiments performed on molecules and molecular systems. These experiments are normally not performed on molecules alone in a vacuum, but molecules in an environment. There is no doubt that the environment, for instance a solvent or a protein, is affecting the properties of the molecules under study. However, the use of quantum mechanical methods is mandatory when calculating many molecular properties, such as the absorption of photons, and the main limitation of modern quantum mechanical methods is the computational cost when doing calculations on medium to large size systems. When the size of the system (number of atoms) is increasing, the computational time increases tremendously due to the scaling of these methods.

An aim of the work behind this thesis has been to reduce the gap between theory and experiments by making it possible to perform advanced quantum mechanical calculations on chromophores in complex systems. This has been made possible by the use of so-called “focused methods”. In short, the part of the system that are of most interest is treated at a high-level theory, that is quantum mechanics, and the surroundings are treated at a much coarser level, with a polarizable embedding.

The introduction to this thesis is organized as follows. The theoretical framework of ground-state quantum mechanics is presented in Chapter 1, the polarizable embedding methods used in this thesis are introduced in Chapter 2, and the theory behind the calculations of molecular electronic properties are presented in Chapter 3. In the end there are summaries of the papers in this thesis (Chapter 4).

Chapter 1

Ground-state quantum mechanics

In this chapter the basic concept of nonrelativistic quantum chemistry for the ground-state will be introduced¹, with a special emphasis on Kohn-Sham density functional theory (KS-DFT, Section 1.3).

1.1 Wavefunctions and Schrödinger equations

In quantum mechanics, the electrons in a molecule can be described by an N -electron wavefunction $\Psi(\mathbf{r}_1, \mathbf{r}_2, \dots, \mathbf{r}_N, t)$, where \mathbf{r}_n is related to the coordinates of electron n as well as its spin. According to one of the postulates of quantum mechanics, the wavefunction has to fulfill (and therefore can be determined by) the time-dependent Schrödinger equation²

$$\hat{H}\Psi(\mathbf{r}_1, \mathbf{r}_2, \dots, \mathbf{r}_N, t) = i\frac{\partial}{\partial t}\Psi(\mathbf{r}_1, \mathbf{r}_2, \dots, \mathbf{r}_N, t) \quad (1.1)$$

¹Hartree atomic units ($\hbar = e = m = 1$) are used throughout this thesis if not stated otherwise.

²E. Schrödinger, *Phys. Rev.*, 1926, **28**, 1049–1070.

where \hat{H} is the Hamiltonian of the molecule. Within the Born-Oppenheimer approximation^{3,4} and without taking into account relativity, the time-dependent Schrödinger equation for a molecule can be expressed with a Hamiltonian consisting of one-electron (\hat{h}) and two-electron (\hat{g}) operators

$$\begin{aligned}\hat{H} &= \sum_{n>m} \hat{V}_{nm} + \sum_i \hat{T}_i + \sum_{i,m} \hat{V}_{im} + \sum_{i>j} \hat{V}_{ij} \\ &= h_{\text{nuc}} + \hat{h} + \hat{g}\end{aligned}\quad (1.2)$$

where the first sum (h_{nuc}) is the repulsion between the nuclei. The second and third sums (collected in \hat{h}) are over all the electrons, and include the kinetic energies of the electrons (\hat{T}_i) as well as the attraction between electrons and nuclei (\hat{V}_{im}). The last sum takes into account the interaction energies between all pairs of electrons. In the second quantization formalism⁵ the electronic terms of the Hamiltonian operator can be expressed as⁶

$$\hat{h} = \sum_{pq} h_{pq} \hat{E}_{pq} \quad (1.3)$$

$$\hat{g} = \sum_{pqrs} g_{pqrs} \hat{e}_{pqrs} \quad (1.4)$$

where the \hat{E}_{pq} and \hat{e}_{pqrs} are the one- and two-electron excitation operators. The singlet excitation operator is defined as

$$\hat{E}_{pq} = a_{p\alpha}^\dagger a_{q\alpha} + a_{p\beta}^\dagger a_{q\beta} \quad (1.5)$$

while \hat{e}_{pqrs} is the two-electron excitation operator, defined as

$$\hat{e}_{pqrs} = a_{p\alpha}^\dagger a_{r\alpha}^\dagger a_{s\alpha} a_{q\alpha} + a_{p\beta}^\dagger a_{r\beta}^\dagger a_{s\beta} a_{q\beta} = \hat{E}_{pq} \hat{E}_{rs} - \delta_{qr} \hat{E}_{ps} \quad (1.6)$$

a^\dagger and a are the creation and annihilation operators, respectively.

³M. Born and R. Oppenheimer, *Ann. Phys.-Berlin*, 1927, **389**, 457–484.

⁴C. Eckart, *Phys. Rev.*, 1934, **46**, 383–387.

⁵V. Fock, *Z. Phys. A: Hadrons Nucl.*, 1932, **75**, 622–647.

⁶T. Helgaker, P. Jørgensen, and J. Olsen, *Molecular Electronic-Structure Theory*, John Wiley & Sons, Ltd, Chichester, 2000.

Equations 1.3 and 1.4 are written as general one-electron and two-electron operators in the second quantization formalism. In the case of the electronic Hamiltonian, the one- and two-electron integrals h_{pq} and g_{pqrs} are given as

$$h_{pq} = \int \phi_p^*(\mathbf{r}) \left(-\frac{1}{2} \nabla^2 \right) \phi_q(\mathbf{r}) d\mathbf{r} - \sum_m Z_m \int \frac{\phi_p^*(\mathbf{r}) \phi_q(\mathbf{r})}{|\mathbf{r} - \mathbf{R}_m|} d\mathbf{r} \quad (1.7)$$

$$g_{pqrs} = \iint \frac{\phi_p^*(\mathbf{r}_1) \phi_q(\mathbf{r}_1) \phi_r^*(\mathbf{r}_2) \phi_s(\mathbf{r}_2)}{|\mathbf{r}_1 - \mathbf{r}_2|} d\mathbf{r}_1 d\mathbf{r}_2 \quad (1.8)$$

where ϕ are the spin-orbitals, and m runs over all nuclei with charge Z_m and position \mathbf{R}_m .

It can be shown, by the separation of variables, that particles in a time-independent potential can be described by the time-independent Schrödinger equation

$$\hat{H} \psi(\mathbf{r}_1, \mathbf{r}_2, \dots, \mathbf{r}_N) = E \psi(\mathbf{r}_1, \mathbf{r}_2, \dots, \mathbf{r}_N). \quad (1.9)$$

where E is the total energy of particles described by the time-independent N -electron wavefunction $\psi(\mathbf{r}_1, \mathbf{r}_2, \dots, \mathbf{r}_N)$.

It is not possible to derive the exact wavefunction for molecules with more than one electron and one nucleus. Therefore, approximate wavefunctions have to be derived. As a first step, the electronic wavefunction can be expressed as molecular orbitals (MO), where there are two electrons in each occupied MO for a closed shell molecule (one with α spin and one with β spin). Each MO can be expanded in terms of functions located on the nuclei, the so-called linear combination of atomic orbital (LCAO) approximation⁷

$$\phi_p^{\text{MO}} = \sum_{\mu} c_{\mu p} \chi_{\mu}^{\text{AO}} \quad (1.10)$$

where χ_{μ}^{AO} is basis function (or atomic orbital) μ , and $c_{\mu p}$ are the molecular orbital coefficients⁸. To ensure that it is antisymmetric and that it fulfils the

⁷J. E. Lennard-Jones, *Trans. Faraday Soc.*, 1929, **25**, 668–686.

⁸All Greek letters, except α and β , are related to atomic orbitals and Latin letters are related to molecular orbitals in the remainder of this section, if not stated otherwise.

Pauli exclusion principle⁹, the wavefunction for a system of N electrons is often written as a linear combination of Slater determinants^{10,11}

$$\psi(\mathbf{r}_1, \mathbf{r}_2, \dots, \mathbf{r}_N) \equiv |0\rangle = \frac{1}{\sqrt{N!}} \begin{vmatrix} \phi_{1\alpha}(\mathbf{r}_1) & \phi_{1\beta}(\mathbf{r}_1) & \cdots & \phi_{\frac{N}{2}\beta}(\mathbf{r}_1) \\ \phi_{1\alpha}(\mathbf{r}_2) & \phi_{1\beta}(\mathbf{r}_2) & \cdots & \phi_{\frac{N}{2}\beta}(\mathbf{r}_2) \\ \vdots & \vdots & \ddots & \vdots \\ \phi_{1\alpha}(\mathbf{r}_N) & \phi_{1\beta}(\mathbf{r}_N) & \cdots & \phi_{\frac{N}{2}\beta}(\mathbf{r}_N) \end{vmatrix} \quad (1.11)$$

where ϕ_n is a molecular orbital, as given in Equation 1.10. In second quantization, on the other hand, the N -electron determinant can be written as a product of creation operators acting on what is called the vacuum state. For a wavefunction with only doubly occupied orbitals, the determinant is written as¹²

$$|0\rangle = \left(\prod_i a_{i\alpha}^\dagger a_{i\beta}^\dagger \right) |vac\rangle \quad (1.12)$$

The antisymmetric property of this wavefunction, and therefore also the Pauli exclusion principle⁹, is fulfilled due to the definition and properties of the creation operator⁶.

One of the cornerstones of quantum chemistry methods is the variational principle. The energy of an approximate wavefunction is higher or equal to the exact ground-state energy¹³. Thus, we can search for the ground-state energy wavefunction by minimizing the expectation value of the Hamiltonian

$$E = \langle 0 | \hat{H} | 0 \rangle \quad (1.13)$$

This is done by finding the minimum of the expectation value by varying the

⁹W. Pauli, *Z. Phys. A: Hadrons Nucl.*, 1925, **31**, 765–783.

¹⁰J. Slater, *Phys. Rev.*, 1929, **34**, 1293–1322.

¹¹The bra-ket notation (P. A. M. Dirac, *Math. Proc. Camb. Philos. Soc.*, 1939, **35**, 416–418) is used in the remainder of this thesis.

¹²The letters i , j and k refer to fully occupied molecular orbitals, while p refers to a general MO.

¹³F. Jensen, *Introduction to Computational Chemistry*, John Wiley & Sons, Ltd, 2007.

molecular orbital coefficients in the wavefunction

$$\frac{\partial \langle 0 | \hat{H} | 0 \rangle}{\partial c_{\mu p}} = 0 \quad (1.14)$$

1.2 Hartree-Fock

In Hartree-Fock theory¹⁴ (HF), the wavefunction is described by a linear combination of determinants, called a configuration state function (CSF)

$$|\text{CSF}\rangle = \sum_i C_i |0\rangle \quad (1.15)$$

where $|0\rangle$ is defined in Equation 1.12. For closed-shell HF, the CSF is a single determinant, thus

$$|\text{CSF}\rangle = \left(\prod_i a_{i\alpha}^\dagger a_{i\beta}^\dagger \right) |vac\rangle \quad (1.16)$$

In the Roothaan formulation of HF theory¹⁵ we will use the atomic orbitals (AOs) given in Equation 1.10 and minimize the energy with respect to the MO coefficients $c_{\mu p}$. The closed-shell HF energy expression is given as one- and two-electron integrals (Eqs. 1.7 and 1.8)

$$E(\mathbf{c}) = 2 \sum_i h_{ii} + \sum_{ij} (2g_{iijj} - g_{ijji}) + h_{\text{nuc}} \quad (1.17)$$

where the subscripts i and j are running over all fully occupied molecular orbitals. The first term represents the kinetic energy of the electrons as well as their attractions to the nuclei, while the second term is the Coulomb interaction (g_{iijj}) between electrons as well as the exchange (g_{ijji}). The last term accounts for the interactions between the nuclei and is constant in the

¹⁴D. R. Hartree, *Math. Proc. Camb. Philos. Soc.*, 1928, **24**, 89-110; V. Fock, *Z. Phys. A: Hadrons Nucl.*, 1930, **61**, 126-148.

¹⁵C. C. J. Roothaan, *Rev. Mod. Phys.*, 1951, **23**, 69-89.

Born-Oppenheimer approximation. The MOs (ϕ_p in Equation 1.10) have to fulfill the following condition during the optimization

$$\langle \phi_i | \phi_j \rangle = \delta_{ij}. \quad (1.18)$$

That is, all the MOs have to be orthonormal. A way of achieving this is to introduce the Hartree-Fock Lagrangian

$$L(\mathbf{c}) = E(\mathbf{c}) - 2 \sum_{ij} \lambda_{ij} (\langle \phi_i | \phi_j \rangle - \delta_{ij}) \quad (1.19)$$

The Lagrangian is then minimized with respect to the elements $c_{\mu k}$, where μ is related to the atomic orbitals, and k is related to the occupied molecular orbitals

$$\frac{\partial L(\mathbf{c})}{\partial c_{\mu k}} = 0 \quad (1.20)$$

In the AO basis we then end up with the following set of equations⁶

$$\sum_{\nu} f_{\mu\nu}^{\text{AO}} c_{\nu k} = \varepsilon_k \sum_{\nu} S_{\mu\nu} c_{\nu k} \quad (1.21)$$

for all occupied molecular orbitals k . These HF equations (Eq. 1.21) can be written in matrix form as

$$\mathbf{f}^{\text{AO}} \mathbf{c} = \mathbf{S} \mathbf{c} \boldsymbol{\varepsilon} \quad (1.22)$$

where $\boldsymbol{\varepsilon}$ is a diagonal matrix containing the orbital energies. The elements of the Fock matrix $f_{\mu\nu}^{\text{AO}}$, in AO basis, are

$$f_{\mu\nu}^{\text{AO}} = h_{\mu\nu} + \sum_{\rho\sigma} D_{\rho\sigma}^{\text{AO}} \left(g_{\mu\nu\rho\sigma} - \frac{1}{2} g_{\mu\sigma\rho\nu} \right) \quad (1.23)$$

where $D_{\rho\sigma}^{\text{AO}}$ is the one-electron density matrix in AO basis, and given by

$$D_{\rho\sigma}^{\text{AO}} = 2 \sum_i c_{\rho i} c_{\sigma i} \quad (1.24)$$

In other words, one HF equation depends on all the other molecular orbital coefficients ($c_{\mu k}$) and we have to solve this problem iteratively. In the most

basic approach the matrix \mathbf{c} from iteration $n - 1$ is used to calculate $D_{\rho\sigma}^{\text{AO}}$ (Eq. 1.24), which then are used to calculate $f_{\mu\nu}^{\text{AO}}$ (Eq. 1.23). A new set of \mathbf{c} is derived by diagonalizing the Fock matrix \mathbf{f}^{AO} (see Equation 1.22). This is done until convergence. In practice, more sophisticated methods are used to improve the convergence. The most widely used is the Direct Inversion of Iterative Subspace (DIIS) method¹⁶.

The HF wavefunction is in many cases not accurate enough to describe molecular systems and molecular properties, but is the starting point for several other more advanced and accurate methods, such as coupled-cluster¹⁷, configuration interaction and Møller-Plesset perturbation theory¹⁸. More importantly for this thesis, the methods and mathematical derivations can easily be transferred to density functional theory.

1.3 Density Functional Theory

Density functional theory (DFT) is by far the most popular and widely used method in quantum chemistry today¹⁹. The main reason is the low computational cost compared to other methods, such as coupled-cluster, but at the same time giving results of comparable accuracy²⁰. A brief introduction to DFT is presented in this section.

For a general external potential, the non-relativistic Hamiltonian for N in-

¹⁶P. Pulay, *Chem. Phys. Lett.*, 1980, **73**, 393-398; P. Pulay, *J. Comput. Chem.*, 1982, **3**, 556-560.

¹⁷J. Čížek, *J. Chem. Phys.*, 1966, **45**, 4256; J. Paldus, J. Čížek, and I. Shavitt, *Phys. Rev. A*, 1972, **5**, 50-67.

¹⁸C. Møller and M. S. Plesset, *Phys. Rev.*, 1934, **46**, 618-622.

¹⁹J. P. Perdew and A. Ruzsinszky, *Int. J. Quantum Chem.*, 2010, **110**, 2801-2807.

²⁰M. Swart and J. G. Snijders, *Theor. Chem. Acc.*, 2003, **110**, 34-41; P. Sałek, T. Helgaker, O. Vahtras, H. Ågren, D. Jonsson, and J. Gauss, *Mol. Phys.*, 2005, **103**, 439-450.

interacting electrons is given as

$$\hat{H} = -\frac{1}{2} \sum_i \nabla_i^2 + \sum_i v(\mathbf{r}_i) + \frac{1}{2} \sum_{i \neq j} \frac{1}{|\mathbf{r}_i - \mathbf{r}_j|} \quad (1.25)$$

According to the Hohenberg-Kohn theorem²¹ there is a one-to-one relationship between the electronic density and an external potential. In other words, for a given potential $v(\mathbf{r})$ there is only one electronic density $\rho(\mathbf{r})$, and *vice versa*. For molecules, this external potential is the Coulomb attractions from all the nuclei

$$v(\mathbf{r}) = - \sum_m \frac{Z_m}{|\mathbf{r} - \mathbf{R}_m|} \quad (1.26)$$

Since the electronic density determines the number of electrons by integration, as well as the positions and charges of the nuclei (and consequently also the Hamiltonian \hat{H} in Equation 1.25), the ground-state energy can be uniquely determined by the electron density²¹. More general, all properties that can be determined by the the Hamiltonian can be determined by the density²². The energy as a functional of the electronic density ρ is given as

$$E[\rho] = \int \rho(\mathbf{r})v(\mathbf{r}) d\mathbf{r} + T[\rho] + V[\rho] \quad (1.27)$$

where the nuclear repulsion term is known, while the kinetic energy density functional ($T[\rho]$) and the electron repulsion density functional ($V[\rho]$) are unknown. Kohn and Sham²³ suggested to extract two large contributions from these two unknown functionals and add a new unknown functional. $T[\rho]$ is replaced by the kinetic energy of non-interacting electrons $T_s[\rho]$, and $V[\rho]$ is replaced by a classical interaction energy expression. The new and unknown term is called the exchange-correlation energy functional. The energy is then given as

$$E[\rho] = V_{ne}[\rho] + T_s[\rho] + J[\rho] + E_{XC}[\rho] \quad (1.28)$$

²¹P. Hohenberg and W. Kohn, *Phys. Rev.*, 1964, **136**, B864–B871.

²²W. Kohn, A. D. Becke, and R. G. Parr, *J. Phys. Chem.*, 1996, **100**, 12974–12980.

²³W. Kohn and L. Sham, *Phys. Rev.*, 1965, **140**, A1133–A1138.

where $T_s[\rho]$ is the kinetic energies of the non-interacting electrons, $V_{ne}[\rho]$ is the potential energies of the electrons due to the nuclei, and $J[\rho]$ is the Coulomb interaction energy between the electrons. The last term is the exchange-correlation functional, and will be treated in more detail in the following section.

The density can in principle be found by minimizing this energy functional. To achieve this, Kohn and Sham introduced orbitals²³, where the density is given as

$$\rho(\mathbf{r}) = \sum_i^N \phi_i^2(\mathbf{r}) \quad (1.29)$$

The Hamiltonian is then expressed as an Hamiltonian for a system of non-interacting electrons moving in an effective external potential $v_{\text{eff}}(\mathbf{r})$. The Hamiltonian then becomes

$$\hat{H} = - \sum_i^N \frac{1}{2} \nabla_i^2 + \sum_i^N v_{\text{eff}}(\mathbf{r}_i) \quad (1.30)$$

The effective potential is such that the electronic density corresponding to the effective potential $v_{\text{eff}}(\mathbf{r})$ for a system of non-interacting electrons is the same as the density corresponding to interacting electrons in the potential $v(\mathbf{r})$ given in the Hamiltonian (Eq. 1.25). The exact wavefunction is then constructed from one-electron orbitals that are solutions of the Kohn-Sham equations

$$f_i \phi_i(\mathbf{r}) = \epsilon_i \phi_i(\mathbf{r}) \quad (1.31)$$

where the Kohn-Sham operator f_i is

$$f_i = -\frac{1}{2} \nabla_i^2 + v_{\text{eff}}(\mathbf{r}_i) \quad (1.32)$$

The effective potential is given as

$$v_{\text{eff}}(\mathbf{r}) = v(\mathbf{r}) + \frac{\partial J[\rho]}{\partial \rho(\mathbf{r})} + \frac{\partial E_{\text{XC}}[\rho]}{\partial \rho(\mathbf{r})} \quad (1.33)$$

where $v(\mathbf{r})$ is the original potential due to the nuclei, the second term is the Coloumb interaction due to the electronic density, and the last term is the exchange-correlation potential.

1.3.1 The exchange-correlation functionals

Kohn-Sham DFT is, in principle, an exact theory, but the exchange-correlation functional $E_{\text{XC}}[\rho]$ is not known and is therefore the holy grail of DFT. It is probably not possible to get an exact exchange-correlation functional, and there is no systematic way of getting functionals with a higher level of accuracy²², as we are used to for wavefunction based methods with its hierarchy of methods. It should be noted that Perdew and Schmidt introduced a Jacob's ladder²⁴ of exchange-correlation functionals where each step in the ladder brings us closer to DFT heaven²⁵.

Originally, Kohn and Sham suggested to use a local density approximation (LDA) for the exchange-correlation functional²³ that was later refined with the local spin density approximation (LSDA)²⁶. LDA is exact for a uniform electron gas, but the electronic densities in molecules are far from uniform. The L(S)DA approach is therefore in many cases not accurate enough for quantum chemistry²⁷. In the generalized gradient approximation (GGA)²⁸, such as used in the PBE functional²⁹, the gradient of the spin density was included. After the development of GGA, DFT became an interesting method also for chemists¹⁹. Becke later recognized the importance of including some exact Hartree-Fock exchange to the exchange-correlation functional³⁰. The hybrid functional suggested by Becke was then modified by Stephens *et al.*³¹ and giving us by far the most widely used exchange-correlation functional in quantum chemistry today, namely B3LYP. The B3LYP functional is given as

$$E_{\text{XC}}^{\text{B3LYP}} = 0.2E_{\text{x}}^{\text{HF}} + 0.8E_{\text{x}}^{\text{LSDA}} + 0.72\Delta E_{\text{x}}^{\text{B88}} + 0.81E_{\text{c}}^{\text{LYP}} + 0.19E_{\text{c}}^{\text{VWN}} \quad (1.34)$$

²⁴Named after the biblical Jacob's dream about a ladder to heaven (Genesis 28:10-19).

²⁵J. P. Perdew and K. Schmidt, *AIP Conf. Proc.*, 2001, **577**, 1–20.

²⁶U. von Barth and L. Hedin, *J. Phys. B: Solid State Phys.*, 1972, **5**, 1629–1642.

²⁷R. O. Jones and O. Gunnarsson, *Rev. Mod. Phys.*, 1989, **61**, 689–746.

²⁸J. P. Perdew and Y. Wang, *Phys. Rev. B*, 1986, **33**, 8800–8802.

²⁹J. Perdew, K. Burke, and M. Ernzerhof, *Phys. Rev. Lett.*, 1996, **77**, 3865–3868.

³⁰A. D. Becke, *J. Chem. Phys.*, 1993, **98**, 5648–5652.

³¹P. J. Stephens, F. J. Devlin, C. F. Chabalowski, and M. J. Frisch, *J. Phys. Chem.*, 1994, **98**, 11623–11627.

and consist of Hartree-Fock exchange³⁰ (E_x^{HF}), LSDA exchange²⁶ (E_x^{LSDA}) and Becke's gradient corrections to the exchange functional³² (ΔE_x^{B88}) to describe the exchange, and a combination of the Lee-Yang-Parr³³ (E_c^{LYP}) and the Vosko-Wilk-Nusair³⁴ (E_c^{VWN}) correlation functionals to describe the correlation.

The enormous popularity of B3LYP is due to its very good performance, and one of the main goals of the development of new XC functionals is therefore to outperform B3LYP. One successful approach has been methods based on the so-called long-range exchange correction scheme³⁵.

For B3LYP, the amount of Hartree-Fock exchange and LDA (local density approximation) exchange is 0.2 and 0.8 respectively (see Equation 1.34), while for range-separated functionals, the ratio between Hartree-Fock and LDA exchange vary with the distance between the interacting electrons. In short, the long-range exchange correction schemes divide the electron repulsion operator into two terms, namely a short-range and a long-range term. Originally³⁶, the error function was used to separate this operator

$$\frac{1}{r_{12}} = \frac{1 - \text{erf}(\mu r_{12})}{r_{12}} + \frac{\text{erf}(\mu r_{12})}{r_{12}} = \text{SR} + \text{LR} \quad (1.35)$$

where the contribution from LDA exchange E_x^{LDA} goes from one for $r \rightarrow 0$ to zero for $r \rightarrow \infty$, while it is opposite for the Hartree-Fock exchange E_x^{HF} contribution, going from zero to one. This way of separating the functionals did not improve on the B3LYP, so a modification was introduced by adding two

³²A. D. Becke, *Phys. Rev. A*, 1988, **38**, 3098–3100.

³³C. Lee, W. Yang, and R. G. Parr, *Phys. Rev. B*, 1988, **37**, 785–789.

³⁴S. H. Vosko, L. Wilk, and M. Nusair, *Can. J. Phys.*, 1980, **58**, 1200–1211.

³⁵T. Leininger, H. Stoll, H.-J. Werner, and A. Savin, *Chem. Phys. Lett.*, 1997, **275**, 151-160; H. Iikura, T. Tsuneda, T. Yanai, and K. Hirao, *J. Chem. Phys.*, 2001, **115**, 3540; Y. Tawada, T. Tsuneda, S. Yanagisawa, T. Yanai, and K. Hirao, *J. Chem. Phys.*, 2004, **120**, 8425-8433.

³⁶T. Leininger, H. Stoll, H.-J. Werner, and A. Savin, *Chem. Phys. Lett.*, 1997, **275**, 151–160.

more parameters³⁷. In the case of CAM-B3LYP, the amount of HF exchange and LDA exchange are given according to the following function

$$\frac{1}{r_{12}} = \frac{1 - [\alpha + \beta \cdot \text{erf}(\mu r_{12})]}{r_{12}} + \frac{\alpha + \beta \cdot \text{erf}(\mu r_{12})}{r_{12}} \quad (1.36)$$

where the first term is related to the short-range interactions while the second term is related to the long-range interactions. This functional showed improved performance when calculating excitation energies³⁸. The contributions is demonstrated in figure 1.1. In the original work, the parameter α was

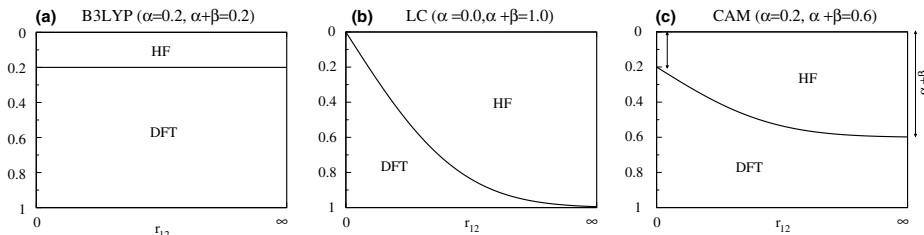


Figure 1.1: The contribution from DFT (LDA) and HF exchange as a function of inter-electronic distance r_{12} for the B3LYP (a), LC (b) and CAM-B3LYP (c) functionals. Reprinted from Yanai *et al.*³⁷ Copyright (2004) with permission from Elsevier

set to 0.2, β was either 0.4, 0.6 or 0.8, and μ was set to 0.33. The calculations in this thesis have been performed with α 0.19 and β 0.46, while μ as for the original CAM-B3LYP article. This corresponds to the values used in the study by Peach *et al.*³⁸.

³⁷T. Yanai, D. P. Tew, and N. C. Handy, *Chem. Phys. Lett.*, 2004, **393**, 51–57.

³⁸M. J. G. Peach, P. Benfield, T. Helgaker, and D. J. Tozer, *J. Chem. Phys.*, 2008, **128**, 044118.

Chapter 2

Polarizable embedding

The two methods discussed so far, Hartree-Fock and KS-DFT, scale formally as N^3 , where N is the number of basis functions (χ in Equation 1.10)³⁹. Therefore, for very large and more realistic molecular systems such as proteins and a molecule solvated in water, purely quantum-mechanical calculations are computationally too demanding. One way of being able to do calculations on such systems is to use a so-called “focused model”. These models separate the system into parts, illustrated in Figure 2.1, and these parts are treated at a different level of theory. The inner region, in our case the solute, is typically treated with quantum mechanics, while the outer region, the solvent, is treated at a much lower level of theory. The inner region will then “feel” the surrounding solvent, which will influence the energy and electronic structure of this solvated QM treated region. If the surrounding solvent is described by a polarizable model, the surrounding will also “feel” the solute.

The simplest way of describing the outer region is with an implicit model,

³⁹The implementations of DFT and HF are scaling as N^2 in most of modern quantum chemistry programs, but also linear scaling has been achieved. See for instance C. Ochsenfeld, J. Kussmann, and D. S. Lambrecht, *Rev. Comput. Chem.*, 2007, **23**, 1-82.

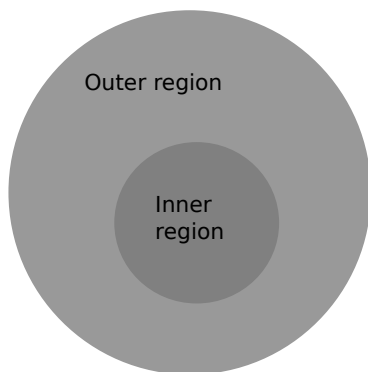


Figure 2.1: The principle of the focused models

where for instance the environment is treated as a dielectric continuum and not as individual particles⁴⁰. Two of the main benefits of this approach are that it takes into account long-range electrostatic interactions and that the dynamics of the system is taken care of by the method. Besides, partly because the dynamics is included implicitly, the overall computational cost is normally much lower than explicit models. The main disadvantage of the continuum compared to explicit models is the lack of specific solute-solvent interactions, for instance hydrogen bonds. A way to circumvent the latter is to include some of the solvent molecules closest to the solute into the quantum-mechanical treated region⁴¹. This requires that we reintroduce the dynamics of the system by, for instance, molecular dynamics calculations since there will no longer be an implicit treatment of the dynamics of the system.

In the explicit models, the outer region is described as discrete particles, such as water molecules in the case of a molecule solvated in water. These particles are typically described with classical molecular mechanics (MM)⁴², and will take into account the specific electrostatic interactions with the quantum-

⁴⁰J. G. Kirkwood, *J. Chem. Phys.*, 1934, **2**, 351; L. Onsager, *J. Am. Chem. Soc.*, 1936, **58**, 1486-1493; J. Tomasi, B. Mennucci, and R. Cammi, *Chem. Rev.*, 2005, **105**, 2999-3093.

⁴¹J. Kongsted and B. Mennucci, *J. Phys. Chem. A*, 2007, **111**, 9890-9900.

⁴²A. Warshel and M. Levitt, *J. Mol. Biol.*, 1976, **103**, 227-249.

mechanically described solute. In such QM/MM methods, the dynamics of the system has to be dealt with, and can for instance be introduced by molecular dynamics⁴³. This normally requires QM/MM calculations on a large number of molecular structures, making it much more computationally expensive than dielectric continuum models.

Another discrete description of the solvent, which will only be mentioned briefly, is quantum-mechanical-based methods. The system is divided into fragments and each fragment is treated at the same level. The interactions between each fragment is then treated by different techniques depending on the method. An example of such a method is the fragment molecular orbital method (FMO)⁴⁴. A benefit of such methods, besides the much lower computational cost than pure QM calculations because of linear scaling, is the possibilities to do massively parallel calculations⁴⁵.

A common feature of the two solvation models used in this thesis is that they are fully self-consistent polarizable schemes. In short, the surroundings not only affects the quantum mechanically described solute, but the solute also influences the surroundings. This is achieved since the surroundings or embedding are polarizable, therefore the term “polarizable embedding”. A consequence is that the interaction between solute and embedding has to be determined iteratively.

In general, for the solvent methods discussed in this thesis, the gas-phase Hamiltonian is replaced by an effective Hamiltonian

$$\hat{H}_{\text{eff}} = \hat{H}_0 + \hat{v}_{\text{PE}} \quad (2.1)$$

where \hat{H}_0 is the vacuum Hamiltonian and \hat{v}_{PE} is the solute-solvent interaction term. The form of the latter depends on the method.

⁴³B. J. Alder and T. E. Wainwright, *J. Chem. Phys.*, 1959, **31**, 459–466.

⁴⁴K. Kitaura, E. Ikeo, T. Asada, T. Nakano, and M. Uebayasi, *Chem. Phys. Lett.*, 1999, **313**, 701–706.

⁴⁵G. D. Fletcher, D. G. Fedorov, S. R. Pruitt, T. L. Windus, and M. S. Gordon, *J. Chem. Theory Comput.*, 2012, **8**, 75–79.

2.1 The integral equation formalism of the polarizable continuum model

The integral equation formalism of the polarizable continuum model (IEF-PCM)⁴⁶ is based on the original PCM method⁴⁷. In the PCM methods, the solvent is implicitly described by a cavity surrounding the solute and the following equations are then describing the electrostatics between the solute and the solvent⁴⁸

$$-\nabla^2 V(\mathbf{r}) = 4\pi\rho(\mathbf{r}) \quad \text{inside the cavity} \quad (2.2)$$

$$-\epsilon\nabla^2 V(\mathbf{r}) = 0 \quad \text{outside the cavity} \quad (2.3)$$

$V(\mathbf{r})$ is the electrostatic potential due to the charge distribution inside the cavity, $\rho(\mathbf{r})$ is the charge density of the solute, and ϵ is the dielectric constant of the solvent. The right-hand side of Equation 2.3 is zero since we assume that the electron density is zero outside the cavity. The following boundary conditions have to be fulfilled

$$V_{\text{inside}} = V_{\text{outside}} \quad (2.4)$$

$$\left(\frac{\partial V}{\partial n}\right)_{\text{inside}} = \epsilon \left(\frac{\partial V}{\partial n}\right)_{\text{outside}} \quad (2.5)$$

where n is a unit vector pointing outwards and perpendicular to the surface. In other words, there has to be a continuity of the potential across the surface (Eq. 2.4), as well as for the gradient of the field (Eq. 2.5).

IEF-PCM is an apparent surface charge (ASC) method, according to the categories of PCM methods introduced in the review by Tomasi and Persico⁴⁹.

⁴⁶E. Cancès, B. Mennucci, and J. Tomasi, *J. Chem. Phys.*, 1997, **107**, 3032-3041; E. Cancès and B. Mennucci, *J. Math. Chem.*, 1998, **23**, 309-326; J. Tomasi, B. Mennucci, and R. Cammi, *Chem. Rev.*, 2005, **105**, 2999-3093.

⁴⁷E. Miertuš, E. Scrocco, and J. Tomasi, *Chem. Phys.*, 1981, **55**, 117-129.

⁴⁸From the general Poisson equation, see for instance E. Kreyszig, *Advanced Engineering Mathematics*, John Wiley & Sons, Ltd, 1999.

⁴⁹J. Tomasi and M. Persico, *Chem. Rev.*, 1994, **94**, 2027-2094.

In ASC methods, the potential due to the apparent charge on the surface (σ) is given as

$$V_\sigma(\mathbf{r}) = \int \frac{\sigma(\mathbf{s})}{|\mathbf{r} - \mathbf{s}|} d\mathbf{s} \approx \sum_k \frac{\sigma(\mathbf{s}_k)A_k}{|\mathbf{r} - \mathbf{s}_k|} = \sum_k \frac{q_k}{|\mathbf{r} - \mathbf{s}_k|} \quad (2.6)$$

The sum is introduced since the PCM cavity is discretized into tesserae, where A_k is the area of tessera k and s_k the position. A graphical representation of a cavity with its tesseration is given in Figure 2.2.

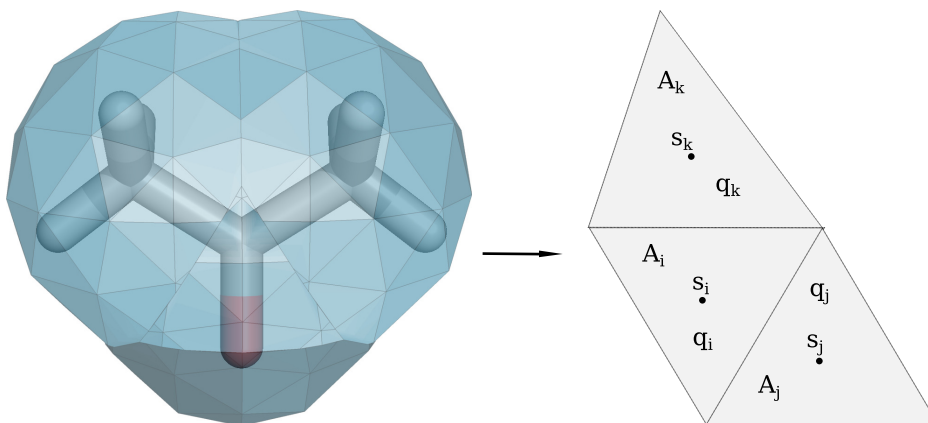


Figure 2.2: To the left: a graphical representation of acetone enclosed in a PCM cavity. To the right: the partition of the cavity into tesserae with the positions s , areas A and surface charges q , as described in the text.

The KS Hamiltonian in the Schrödinger equation (Eq. 1.25) is modified to include the interaction energy between the solute and the apparent charge on the cavity surface. The extra term in the effective solvent Hamiltonian is given as

$$\hat{v}_{\text{PE}} = \sum_k \hat{q}_k \hat{V}_k \quad (2.7)$$

where the sum runs over all tesserae, q_k is the apparent charge on tessera k due to the electrons and nuclei of the solute, while \hat{V}_k is the potential due to the solute. This term can be divided into four terms depending on the origin

of the apparent charges and potentials.

$$\hat{J} = \sum_k \hat{V}_k^e q_k^N = \sum_{pq} J_{pq} \hat{E}_{pq} \quad (2.8a)$$

$$\hat{Y} = \sum_k V_k^N \hat{q}_k^e = \sum_{pq} Y_{pq} \hat{E}_{pq} \quad (2.8b)$$

$$\hat{X} = \sum_k \hat{V}_k^e \hat{q}_k^e = \sum_{pqrs} X_{pqrs} \hat{E}_{pq} \langle 0 | \hat{E}_{rs} | 0 \rangle \quad (2.8c)$$

$$\hat{U}_{NN} = \sum_k V_k^N q_k^N \quad (2.8d)$$

where we once again are using the second quantization formalism. The contributions 2.8a and 2.8b are formally identical, since the potential V is connected to the apparent surface charge q through

$$\mathbf{V} = \mathbf{K} \cdot \mathbf{q} \quad (2.9)$$

where the matrix \mathbf{K} depends on the dielectric constant of the medium and the geometry of the cavity, and \mathbf{V} and \mathbf{q} are vectors where the number of elements equals the number of tesserae. This also means that it is only necessary to know the potential on the cavity surface due to the charge density of the solute to solve the PCM equations. To get the apparent surface charge, \mathbf{K} has to be inverted⁵⁰.

In many situations, PCM and other implicit solvent models fail to describe the interaction between the solute and the solvent, for instance if there are strong hydrogen bonds. The solvent molecules then has to be explicitly included in the system. This can either be done in a super-molecule way, where the molecules closest to the soluted molecule is included in the QM region, while the remaining molecules are included implicitly by PCM, or by using an explicit model with classically treated solvent molecules, thus QM/MM. In the next section, one such polarizable QM/MM method will be presented.

⁵⁰Equation 2.9 can also be solved iteratively. See for instance G. Scalmani, V. Barone, K. N. Kudin, C. S. Pomelli, G. E. Scuseria, and M. J. Frisch, *Theor. Chem. Acc.*, 2004, **111**, 90-100.

2.2 Quantum Mechanics/Molecular Mechanics (QM/MM)

In the quantum mechanics/molecular mechanics (QM/MM) approach, the solvent is treated classically and the potential due to the classical region enters the Hamiltonian of the solute. In one of the simplest versions of QM/MM, the solvent is described by partial point charges and therefore the method neglects the polarization of the solvent due to the QM region⁵¹. A more realistic description of the environment is obtained by introducing polarizable classical sites⁵².

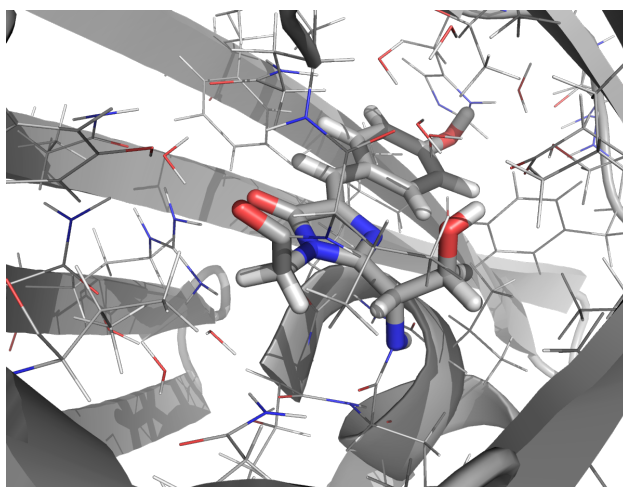


Figure 2.3: An example of the separation of a protein (GFP) into a QM region and a MM region. The QM treated region is represented by sticks, while classically treated embedding is represented by lines and cartoons.

The Kohn-Sham Hamiltonian is modified due to the contributions from the surrounding polarizable embedding with a PE operator consisting of two

⁵¹D. Bakowies and W. Thiel, *J. Phys. Chem.*, 1996, **100**, 10580–10594.

⁵²J. Applequist, J. R. Carl, and K.-K. Fung, *J. Am. Chem. Soc.*, 1972, **94**, 2952-2960; B. Thole, *Chem. Phys.*, 1981, **59**, 341-350.

contributions⁵³

$$\hat{v}_{\text{PE}} = \hat{v}_{\text{PE}}^{\text{es}} + \hat{v}_{\text{PE}}^{\text{ind}}, \quad (2.10)$$

where the first one is the interaction between the static multipoles and the electron density, and the second term is the interaction between the induced dipoles and the electron density. These terms are

$$\hat{v}_{\text{PE}}^{\text{es}} = \sum_{s=1}^S \sum_{k=0}^K \frac{(-1)^{(k)}}{k!} \mathbf{Q}_s^{(k)} \hat{\mathbf{F}}_{s,\text{el}}^{(k)} \quad (2.11)$$

$$\hat{v}_{\text{PE}}^{\text{ind}} = - \sum_{s=1}^S \boldsymbol{\mu}_s^{\text{ind}} \hat{\mathbf{F}}_{s,\text{el}}^{(1)} \quad (2.12)$$

where the sums over s are over all the classical sites⁵⁴, the sum over k is over the order of the multipole moments ($k = 0$ for charges. $k = 1$ for dipoles etc.). S is the total number of classical sites, and K is the truncation level of the multipole expansion. $\mathbf{Q}_s^{(k)}$ is the k th order multipole moment on site s , that is $\mathbf{Q}_s^{(0)} = q_s$, $\mathbf{Q}_s^{(1)} = \boldsymbol{\mu}_s$ etc. The operator $\hat{\mathbf{F}}_{s,\text{el}}^{(k)}$ is defined as

$$\hat{\mathbf{F}}_{s,\text{el}}^{(k)} = \sum_{pq} t_{s,pq}^{(k)} \hat{E}_{pq} \quad (2.13)$$

where \hat{E}_{pq} is, as always, the single excitation operator given in Equation 1.5, and $t_{s,pq}^{(k)}$ is

$$t_{s,pq}^{(k)} = - \int \rho_{pq}(\mathbf{r}) \mathbf{T}_s^{(k)}(\mathbf{r}) d\mathbf{r} \quad (2.14)$$

$\mathbf{T}_s^{(k)}(\mathbf{r})$ is the interaction tensor⁵⁵, written as

$$\mathbf{T}_s^{(k)}(\mathbf{r}) = \nabla^k \frac{1}{|\mathbf{r} - \mathbf{R}_s|} \quad (2.15)$$

⁵³The remainder of this section is based on the work and derivation of Kongsted and co-workers: J. M. Olsen, K. Aidas, and J Kongsted, *J. Chem. Theory Comput.*, 2010, **6**, 3721-3734, J. M. H. Olsen and J. Kongsted, *Adv. Quantum Chem.*, 2011, **61**, 107-143.

⁵⁴The sums over s in Equations 2.11 and 2.12 are not necessarily over the same s . In other words, the multipole moments and the induced dipoles do not have to be located on the same classical sites.

⁵⁵A. J. Stone, *The Theory of Intermolecular Forces*, Oxford University Press, 1996.

The induced dipole on each classical site ($\boldsymbol{\mu}_s^{\text{ind}}$) is given as⁴²

$$\boldsymbol{\mu}_s^{\text{ind}} = \boldsymbol{\alpha}_s \mathbf{F}_s \quad (2.16)$$

where $\boldsymbol{\alpha}_s$ is the (isotropic or anisotropic) polarizability and \mathbf{F}_s is the local electric field on site s . The electric field is due to the nuclei and electrons in the quantum-mechanically described region, as well as due to the permanent multipoles and induced dipoles on the other classic sites

$$\mathbf{F}_s = \mathbf{F}_{\text{nuc}} + \mathbf{F}_{\text{el}} + \mathbf{F}_{\text{mul}} + \mathbf{F}_{\text{ind}} \quad (2.17)$$

The induced dipole moments are also depending on all the other induced dipole moments, so Equation 2.16 has to be solved iteratively or directly by a matrix-vector multiplication

$$\boldsymbol{\mu}^{\text{ind}} = \mathbf{A}^{-1} \mathbf{F} \quad (2.18)$$

The matrix \mathbf{A} is of size $3N \times 3N$, where N is the number of classical sites, and given as⁵⁶

$$\mathbf{A} = \begin{bmatrix} \boldsymbol{\alpha}_1^{-1} & \mathbf{T}_{12}^{(2)} & \cdots & \mathbf{T}_{1N}^{(2)} \\ \mathbf{T}_{21}^{(2)} & \boldsymbol{\alpha}_2^{-1} & \ddots & \vdots \\ \vdots & \ddots & \ddots & \mathbf{T}_{(N-1)N}^{(2)} \\ \mathbf{T}_{N1}^{(2)} & \cdots & \mathbf{T}_{N(N-1)}^{(2)} & \boldsymbol{\alpha}_N^{-1} \end{bmatrix} \quad (2.19)$$

$\boldsymbol{\alpha}_a$ are the polarizability tensors for the classical sites and the interaction tensors $\mathbf{T}_{ab}^{(2)}$ are given in Equation 2.15⁵⁷. Since the induced dipoles depend on the electric field from the electron density, the interaction operator between the electronic density and the induced dipoles has to be updated in every SCF iteration. Thus, the polarization is treated self-consistently.

⁵⁶J. Applequist, J. R. Carl, and K.-K. Fung, *J. Am. Chem. Soc.*, 1972, **94**, 2952–2960.

⁵⁷Equation 2.15 refers to the interaction between the electron density and a multipole moment, while the interaction tensors in equation 2.19 refer to the interaction between two induced dipoles.

The contribution from the polarizable QM/MM embedding to the total DFT energy, analogous to the contribution to the KS Hamiltonian, consists of two extra terms in addition to the original pure DFT term

$$E_{\text{tot}}^{\text{PE}} = E_{\text{DFT}}^{\text{PE}} + E_{\text{es}}^{\text{PE}} + E_{\text{ind}}^{\text{PE}} \quad (2.20)$$

The first term $E_{\text{DFT}}^{\text{PE}}$ is the energy of the isolated QM-treated region, $E_{\text{es}}^{\text{PE}}$ is the contribution to the energy due to the interaction between the multipoles and the QM region, while $E_{\text{ind}}^{\text{PE}}$ is the energy contribution due to the interaction between the induced dipole moments on the classical sites and electronic charges, nuclear charges and static multipole moments. One important point is that, even if the energy is separated into QM and QM/MM contributions, the energy term $E_{\text{DFT}}^{\text{PE}}$ is not independent of the PE potential. This means that the DFT energy calculated without the surrounding embedding will not be identical to the $E_{\text{DFT}}^{\text{PE}}$ energy term. The reason is that the electronic distribution, and therefore consequently the energy, is changed due to the extra potential from the classical region.

The contribution to the energy due to the interaction between the quantum-mechanically described solute and the multipoles are given as

$$E_{\text{es}}^{\text{PE}} = \sum_{s=1}^S \sum_{k=0}^K \frac{(-1)^k}{k!} \left(\mathbf{F}_{s,\text{nuc}}^{(k)} + \langle 0 | \hat{\mathbf{F}}_{s,\text{el}}^{(k)} | 0 \rangle \right) \mathbf{Q}_s^{(k)} \quad (2.21)$$

resembling the static multipole contribution to the KS Hamiltonian (Eq. 2.11), except that the interactions between the multipoles and nuclei (m with charge Z_m) are included, and that the contribution from the electron-multipole interaction is given as an expectation value of the $\hat{\mathbf{F}}_{s,\text{el}}^{(k)}$ operator, defined in Equation 2.13. The nuclear contribution is defined as

$$\mathbf{F}_{s,\text{nuc}}^{(k)} = \sum_m^M Z_m \mathbf{T}_{m,s}^{(k)}(\mathbf{R}_m) \quad (2.22)$$

where $\mathbf{T}_{ms}^{(k)}(\mathbf{R}_m)$ is the interaction tensor (Eq. 2.15) between the nucleus m and multipole moment s of order k . The energy contribution due to the

interaction between the induced dipoles and the quantum-mechanical region, as well as with the static multipole moments, are given as

$$E_{\text{ind}}^{\text{PE}} = -\frac{1}{2} \sum_s^S (\mathbf{F}_{\text{nuc}} + \mathbf{F}_{\text{el}} + \mathbf{F}_{\text{mul}}) \boldsymbol{\mu}_s^{\text{ind}} \quad (2.23)$$

where, as for the contribution to the KS Hamiltonian (Eq. 2.12), the induced dipole moments are induced by the total electric field, given in Equation 2.17.

From a computational point of view, the way the polarizations are derived in the PCM and QM/MM polarizable embedding schemes are very similar. In the case of PCM, the apparent charges due to the potential from all electrons and nuclei are calculated for every tesserae, while for QM/MM, the induced dipoles due to the electric field at every classical site from the electrons and nuclei of the solute are calculated. The apparent surface charge for PCM can be obtained by solving Equation 2.9 (page 20), while the induced dipoles for QM/MM can be obtained by solving Equation 2.18 (page 23). In both cases it is necessary to invert an often large matrix that depends on fixed parameters, or iteratively solve a set of linear equations. The matrix \mathbf{K} in Equation 2.18 (PCM) depends, as mentioned before, on the cavity structure and the dielectric constant of the medium, and the matrix \mathbf{A} in Equation 2.19 (QM/MM) depends on the polarization of the classical sites and their positions.

Chapter 3

Molecular Electronic Properties

3.1 Time-dependent DFT

The Hohenberg-Kohn theorems, as discussed in Section 1.3, are only valid for ground-state energies⁵⁸. In time-dependent DFT we instead have the Runge-Gross theorem that states that there is a one-to-one correspondence between a time-dependent external potential and a time-dependent electronic density, up to a time-independent constant⁵⁹.

The time-dependent Kohn-Sham equation for a system $|t\rangle$ exposed to an external potential $\hat{V}(t)$ is given as

$$\left(\hat{H}(t) + \hat{V}(t)\right) |t\rangle = i \frac{\partial}{\partial t} |t\rangle \quad (3.1)$$

$V(t)$ is a small perturbation to the time-dependent KS Hamiltonian, where the time-dependent KS Hamiltonian is given as

$$\hat{H}(t) = \sum_{pq} f_{pq}(t) \hat{E}_{pq} \quad (3.2)$$

⁵⁸R. Gaudoin and K. Burke, *Phys. Rev. Lett.*, 2004, **93**, 173001.

⁵⁹E. Runge and E. K. U. Gross, *Phys. Rev. Lett.*, 1984, **52**, 997–1000.

$f_{pq}(t)$ is the KS operator defined in Equation 1.32, except that the Coloumb interaction term j_{pq} and the exchange-correlation term $v_{xc,pq}$ now are time-dependent

$$f_{pq}(t) = h_{pq} + j_{pq}(t) + v_{xc,pq}(t) \quad (3.3)$$

since they depend on the time-dependent density. The two first terms are known and “simple”. The third term is, as for ground-state DFT, a complex functional including many-body effects that are not included in the two other terms. In most cases, and also in this thesis, the adiabatic approximation⁶⁰ is used. In the adiabatic approximation, the same functionals as for the time-independent KS-DFT are used, as well as a time-independent density at fixed time⁶¹.

3.2 Response theory

Response theory is a way to derive molecular properties with the use of perturbation theory⁶². In this work, the properties calculated are the one-photon and two-photon absorption (OPA and TPA). That is, the excitation of electrons due to the absorption of one photon, or the absorption of two photons simultaneously⁶³. The absorption of photons will only happen if the energy of a photon matches the energy difference between two quantum states of the molecular system, or, in the case of TPA, if the total energy of two photons matches the energy difference between two quantum states of the molecular system.

The first step is to look at the expectation value of a time-independent operator \hat{A} for a time-dependent system $|t\rangle$, and then expand this expectation

⁶⁰R. Bauernschmitt and R. Ahlrichs, *Chem. Phys. Lett.*, 1996, **256**, 454–464.

⁶¹R. E. Stratmann, G. E. Scuseria, and M. J. Frisch, *J. Chem. Phys.*, 1998, **109**, 8218–8224.

⁶²J. Olsen and P. Jørgensen, *J. Chem. Phys.*, 1985, **82**, 3235–3264.

⁶³M. Göppert-Mayer, *Ann. Phys.-Berlin*, 1931, **401**, 273–294.

value in orders of the perturbation

$$\langle t|\hat{A}|t\rangle = \langle t|\hat{A}|t\rangle^{(0)} + \langle t|\hat{A}|t\rangle^{(1)} + \langle t|\hat{A}|t\rangle^{(2)} + \dots \quad (3.4)$$

The first term is the expectation value for the unperturbed wavefunction, $\langle 0|\hat{A}|0\rangle$. The second and third terms describe the linear and quadratic response to the perturbation, respectively, and can be written in a Fourier transform representation as

$$\langle t|\hat{A}|t\rangle^{(1)} = \int \langle\langle \hat{A}; \hat{V}^\omega \rangle\rangle_\omega e^{-i\omega t} d\omega \quad (3.5)$$

$$\langle t|\hat{A}|t\rangle^{(2)} = \frac{1}{2} \iint \langle\langle \hat{A}; \hat{V}^{\omega_1}, \hat{V}^{\omega_2} \rangle\rangle_{\omega_1, \omega_2} e^{-i(\omega_1 + \omega_2)t} d\omega_1 d\omega_2 \quad (3.6)$$

These expressions are the so-called response functions⁶², where $\langle\langle \hat{A}; \hat{V}^\omega \rangle\rangle_\omega$ is the linear response function, and $\langle\langle \hat{A}; \hat{V}^{\omega_1}, \hat{V}^{\omega_2} \rangle\rangle_{\omega_1, \omega_2}$ is the quadratic response function.

The linear response function contains poles at resonance frequencies and will therefore diverge for frequencies close to resonance of an electronic transition⁶⁴. This is easily seen if the response functions are derived for an exact state. Then we get the following linear response function⁶²

$$\langle\langle \hat{A}; \hat{V}^\omega \rangle\rangle_\omega = \sum_{k>0} \left(\frac{\langle 0|\hat{A}|k\rangle \langle k|\hat{V}^\omega|0\rangle}{\omega - \omega_k} - \frac{\langle 0|\hat{A}|k\rangle \langle k|\hat{V}^\omega|0\rangle}{\omega + \omega_k} \right) \quad (3.7)$$

where the sum k runs over all excited states $|k\rangle$, and the frequencies $\omega_k = E_n - E_0$. The linear response function will have poles at $\omega = \omega_k$, thus at the excitation energies for one-photon absorption. The oscillator strength of an electronic transition with frequency ω_k is given as

$$f_{0k} = \frac{2}{3\omega_k} S_\alpha \quad (3.8)$$

where α is one of the three Cartesian directions (x , y or z). The dipole transition strength S_α is given as the residue of the linear response function⁶⁵,

⁶⁴P. Norman, *Phys. Chem. Chem. Phys.*, 2011, **13**, 20519–20535.

⁶⁵Jeppe Olsen and Poul Jørgensen, in *Modern Electronic Structure Theory*, ed. David R. Yarkony, World Scientific, 1995, ch. 13, pp. 857–990.

with the operators \hat{A} and \hat{V}^ω equal the electric dipole operator

$$S_\alpha = \lim_{\omega \rightarrow \omega_k} (\omega - \omega_k) \langle\langle \hat{\mu}_\alpha; \hat{\mu}_\alpha \rangle\rangle_\omega = \langle 0 | \hat{\mu}_\alpha | k \rangle \langle k | \hat{\mu}_\alpha | 0 \rangle \quad (3.9)$$

Similarly, The two-photon absorption properties are obtained from the poles in the quadratic response functions. The two-photon absorption cross section for linearly polarized light is given, in atomic units, as

$$\delta_{\text{au}}^{\text{TPA}} = \frac{1}{15} \sum_{\alpha, \beta} [S_{\alpha\alpha} S_{\beta\beta}^* + S_{\alpha\beta} S_{\alpha\beta}^* + S_{\alpha\beta} S_{\beta\alpha}^*], \quad (3.10)$$

where the two photon transition matrix element $S_{\alpha\beta}$ for absorption of two photons with identical energies is given by the residue of the quadratic response function

$$S_{\alpha\beta} = \sum_{n>0} \left(\frac{\langle 0 | \hat{\mu}_\alpha | n \rangle \langle n | \hat{\mu}_\beta | k \rangle}{\omega_n - \omega_k/2} + \frac{\langle 0 | \hat{\mu}_\beta | n \rangle \langle n | \hat{\mu}_\alpha | k \rangle}{\omega_n - \omega_k/2} \right). \quad (3.11)$$

3.2.1 KS-DFT response functions

In this section we will derive explicit expression for the response functions for a case of KS-DFT⁶⁶. The time-dependent KS determinant can be written with an exponential parametrization as

$$|t\rangle = e^{-\hat{\kappa}(t)} |0\rangle \quad (3.12)$$

where $|0\rangle$ is the time-independent, unperturbed KS determinant, and $\hat{\kappa}(t)$ is the time-evolution operator. The time-evolution operator is given as

$$\hat{\kappa}(t) = \sum_{pq} \kappa_{pq}(t) \hat{E}_{pq} \quad (3.13)$$

⁶⁶The formalism used in this section is mainly based on the work by Salek *et al.*: P. Salek, O. Vahtras, T. Helgaker, and H. Ågren, *J. Chem. Phys.*, 2002, **117**, 9630-9645.

where \hat{E}_{pq} is the excitation operator (Eq. 1.5). The time-dependent density is given as the expectation value of the density operator $\hat{\rho}(\mathbf{r})$

$$\rho(\mathbf{r}, t) = \langle t | \hat{\rho}(\mathbf{r}) | t \rangle = \langle 0 | e^{\hat{\kappa}(t)} \hat{\rho}(\mathbf{r}) e^{-\hat{\kappa}(t)} | 0 \rangle \quad (3.14)$$

where the density operator is given as

$$\hat{\rho}(\mathbf{r}) = \sum_{pq} \phi_p^*(\mathbf{r}) \phi_q(\mathbf{r}) \hat{E}_{pq} \quad (3.15)$$

The expression for the density can be expanded with a Baker-Campbell-Hausdorff (BCH) expansion

$$\rho(\mathbf{r}, t) = \rho(\mathbf{r}, 0) + \langle 0 | [\hat{\kappa}(t), \hat{\rho}(\mathbf{r})] | 0 \rangle + \frac{1}{2} \langle 0 | [\hat{\kappa}(t), [\hat{\kappa}(t), \hat{\rho}(\mathbf{r})]] | 0 \rangle + \dots \quad (3.16)$$

The time-evolution operator in Equation 3.13 can be expanded as

$$\hat{\kappa}(t) = \hat{\kappa}^{(1)}(t) + \hat{\kappa}^{(2)}(t) + \dots \quad (3.17)$$

The latter expansion is used in Equation 3.16 and we get

$$\begin{aligned} \rho(\mathbf{r}, t) = \rho(\mathbf{r}, 0) + \langle 0 | [\hat{\kappa}^{(1)}(t), \hat{\rho}(\mathbf{r})] | 0 \rangle + \langle 0 | [\hat{\kappa}^{(2)}(t), \hat{\rho}(\mathbf{r})] | 0 \rangle \\ + \langle 0 | [\hat{\kappa}^{(1)}(t), [\hat{\kappa}^{(1)}(t), \hat{\rho}(\mathbf{r})]] | 0 \rangle + \dots \end{aligned} \quad (3.18)$$

Collecting zeroth-, first- and second-order terms, and using Equation 3.15, we get the zeroth-, first- and second-order perturbed densities

$$\rho^{(0)}(\mathbf{r}, t) = \sum_{pq} \phi_p^*(\mathbf{r}) \phi_q(\mathbf{r}) \langle 0 | \hat{E}_{pq} | 0 \rangle = \sum_{pq} \phi_p^*(\mathbf{r}) \phi_q(\mathbf{r}) D_{pq}^{(0)} \quad (3.19)$$

$$\rho^{(1)}(\mathbf{r}, t) = \sum_{pq} \phi_p^*(\mathbf{r}) \phi_q(\mathbf{r}) \langle 0 | [\hat{\kappa}^{(1)}, \hat{E}_{pq}] | 0 \rangle = \sum_{pq} \phi_p^*(\mathbf{r}) \phi_q(\mathbf{r}) D_{pq}^{(1)} \quad (3.20)$$

$$\begin{aligned} \rho^{(2)}(\mathbf{r}, t) &= \sum_{pq} \phi_p^*(\mathbf{r}) \phi_q(\mathbf{r}) \left(\langle 0 | [\hat{\kappa}^{(2)}, \hat{E}_{pq}] | 0 \rangle + \frac{1}{2} \langle 0 | [\hat{\kappa}^{(1)}, [\hat{\kappa}^{(1)}, \hat{E}_{pq}]] | 0 \rangle \right) \\ &= \sum_{pq} \phi_p^*(\mathbf{r}) \phi_q(\mathbf{r}) D_{pq}^{(2)} \end{aligned} \quad (3.21)$$

where the perturbed density matrices have been introduced ($D_{pq}^{(0)}$, $D_{pq}^{(1)}$ and $D_{pq}^{(2)}$). The time-dependent KS Hamiltonian can be expanded in orders of the perturbation, n , as well, since it depends on the functionals of the density

$$\hat{H}(t) = \sum_n \sum_{pq} (\delta_{0n} h_{pq} + j_{pq}^{(n)} + v_{xc,pq}^{(n)}) \hat{E}_{pq} \quad (3.22)$$

The time-dependent KS determinant (Eq. 3.12) can be used to write the expectation value of the time-independent operator \hat{A}

$$\langle t | \hat{A} | t \rangle = \langle 0 | e^{\hat{\kappa}(t)} \hat{A} e^{-\hat{\kappa}(t)} | 0 \rangle \quad (3.23)$$

This expectation value can be expanded by the use of a BCH expansion, as in Equation 3.16

$$\langle 0 | e^{\hat{\kappa}(t)} \hat{A} e^{-\hat{\kappa}(t)} | 0 \rangle = \langle 0 | \hat{A} | 0 \rangle + \langle 0 | [\hat{\kappa}(t), \hat{A}] | 0 \rangle + \frac{1}{2} \langle 0 | [\hat{\kappa}(t), [\hat{\kappa}(t), \hat{A}]] | 0 \rangle + \dots \quad (3.24)$$

An expansion of the time-evolution operator up to second-order (Eq. 3.17) is then inserted into Equation 3.24

$$\begin{aligned} \langle 0 | e^{\hat{\kappa}(t)} \hat{A} e^{-\hat{\kappa}(t)} | 0 \rangle &= \langle 0 | \hat{A} | 0 \rangle \\ &+ \langle 0 | [\hat{\kappa}^{(1)}(t), \hat{A}] | 0 \rangle + \langle 0 | [\hat{\kappa}^{(2)}(t), \hat{A}] | 0 \rangle \\ &+ \frac{1}{2} \langle 0 | [\hat{\kappa}^{(1)}(t), [\hat{\kappa}^{(1)}(t), \hat{A}]] | 0 \rangle + \frac{1}{2} \langle 0 | [\hat{\kappa}^{(2)}(t), [\hat{\kappa}^{(1)}(t), \hat{A}]] | 0 \rangle \\ &+ \frac{1}{2} \langle 0 | [\hat{\kappa}^{(1)}(t), [\hat{\kappa}^{(2)}(t), \hat{A}]] | 0 \rangle + \dots \end{aligned} \quad (3.25)$$

Since we are only interested in linear and quadratic response properties in this thesis, we will only keep terms that are up to second-order in the perturbation. That is

$$\begin{aligned} \langle 0 | e^{\hat{\kappa}(t)} \hat{A} e^{-\hat{\kappa}(t)} | 0 \rangle &= \langle 0 | \hat{A} | 0 \rangle + \langle 0 | [\hat{\kappa}^{(1)}(t), \hat{A}] | 0 \rangle + \langle 0 | [\hat{\kappa}^{(2)}(t), \hat{A}] | 0 \rangle \\ &+ \frac{1}{2} \langle 0 | [\hat{\kappa}^{(1)}(t), [\hat{\kappa}^{(1)}(t), \hat{A}]] | 0 \rangle \end{aligned} \quad (3.26)$$

This expansion can be divided into zeroth-, first- and second-order terms

$$\langle t|\hat{A}|t\rangle^{(0)} = \langle 0|\hat{A}|0\rangle \quad (3.27)$$

$$\langle t|\hat{A}|t\rangle^{(1)} = \langle 0|[\hat{\kappa}^{(1)}(t), \hat{A}]|0\rangle \quad (3.28)$$

$$\langle t|\hat{A}|t\rangle^{(2)} = \langle 0|[\hat{\kappa}^{(2)}(t), \hat{A}]|0\rangle + \frac{1}{2}\langle 0|[\hat{\kappa}^{(1)}(t), [\hat{\kappa}^{(1)}(t), \hat{A}]]|0\rangle \quad (3.29)$$

By using the Fourier transformed of the $\hat{\kappa}^{(n)}(t)$ operators we end up with the following linear (Eq. 3.30) and quadratic (Eq. 3.31) response functions

$$\langle\langle \hat{A}; \hat{V}^\omega \rangle\rangle_\omega = \langle 0|[\hat{\kappa}^\omega, \hat{A}]|0\rangle \quad (3.30)$$

$$\langle\langle \hat{A}; \hat{V}^{\omega_1}, \hat{V}^{\omega_2} \rangle\rangle_{\omega_1, \omega_2} = \langle 0|[\hat{\kappa}^{\omega_1, \omega_2}, \hat{A}]|0\rangle + \hat{P}_{12}\langle 0|[\hat{\kappa}^{\omega_1}, [\hat{\kappa}^{\omega_2}, \hat{A}]]|0\rangle \quad (3.31)$$

where \hat{P}_{12} is the symmetrizer operator defined as

$$\hat{P}_{12}f(\omega_1, \omega_2) = \frac{1}{2}(f(\omega_1, \omega_2) + f(\omega_2, \omega_1)) \quad (3.32)$$

The next step is to find an expression where we can derive $\hat{\kappa}^\omega$, $\hat{\kappa}^{\omega_1}$, $\hat{\kappa}^{\omega_2}$ and $\hat{\kappa}^{\omega_1, \omega_2}$ in Equations 3.30 and 3.31. The Ehrenfest theorem⁶⁷ can be written as⁶⁸

$$\langle 0| \left[\hat{Q}, e^{\kappa \hat{t}} \left(\hat{H}(t) + \hat{V}(t) - i \frac{d}{dt} \right) e^{-\kappa \hat{t}} \right] |0\rangle = 0 \quad (3.33)$$

where $\hat{H}(t)$ is the perturbed Hamiltonian given in Equation (3.22), and \hat{Q} can be any time-independent one-electron operator. By using a vector $\hat{\mathbf{q}}$ consisting of all the excitation operators \hat{E}_{pq} (Eq. 1.5, page 4) we obtain a set of equations

$$\langle 0| \left[\hat{\mathbf{q}}, e^{\kappa \hat{t}} \left(\hat{H}(t) + \hat{V}(t) - i \frac{d}{dt} \right) e^{-\kappa \hat{t}} \right] |0\rangle = 0 \quad (3.34)$$

Once again we can use a BCH expansion (Eq. 3.16) with the KS Hamiltonian expanded in orders of the perturbation, and collect all terms that are of first- and second-order. The first-order terms are collected as

$$\langle 0|[\hat{\mathbf{q}}, [\hat{\kappa}^{(1)}, \hat{H}^{(0)}] + \hat{H}^{(1)}]|0\rangle + i\langle 0|[\hat{\mathbf{q}}, \hat{\kappa}^{(1)}]|0\rangle = -\langle 0|[\hat{\mathbf{q}}, \hat{V}(t)]|0\rangle \quad (3.35)$$

⁶⁷P. Ehrenfest, *Z. Phys. A: Hadrons Nucl.*, 1927, **45**, 455–457.

⁶⁸P. Salek, O. Vahtras, T. Helgaker, and H. Ågren, *J. Chem. Phys.*, 2002, **117**, 9630–9645.

where the n th-order KS hamiltonian is given as

$$\hat{H}^{(n)} = \sum_{pq} \left(\delta_{0n} h_{pq} + j_{pq}^{(n)} + v_{\text{XC},pq}^{(n)} \right) \hat{E}_{pq} \quad (3.36)$$

and $\hat{V}(t)$ is a first-order term. In the frequency domain, Equation 3.35 becomes

$$\langle 0 | [\hat{\mathbf{q}}, [\hat{\kappa}^\omega, \hat{H}^{(0)}] + \hat{H}^\omega] | 0 \rangle + \omega \langle 0 | [\hat{\mathbf{q}}, \hat{\kappa}^\omega] | 0 \rangle = -\langle 0 | [\hat{\mathbf{q}}, \hat{V}^\omega] | 0 \rangle \quad (3.37)$$

Equation 3.37 is used to find the parameters $\hat{\kappa}^\omega$ for the linear response functions (Eq. 3.30). The second-order terms, in the frequency domain, are

$$\begin{aligned} & \langle 0 | [\hat{\mathbf{q}}, [\hat{H}^{(0)}, \hat{\kappa}^{\omega_1, \omega_2}] - \hat{H}^{\omega_1, \omega_2}] | 0 \rangle - (\omega_1 + \omega_2) \langle 0 | [\hat{\mathbf{q}}, \hat{\kappa}^{\omega_1, \omega_2}] | 0 \rangle \\ & = \hat{P}_{12} \langle 0 | [\hat{\mathbf{q}}, [\hat{\kappa}^{\omega_1}, [\hat{\kappa}^{\omega_2}, \hat{H}^{(0)}]] + 2[\hat{\kappa}^{\omega_1}, \hat{V}^{\omega_2} + \hat{H}^{\omega_2}] + \omega_2[\hat{\kappa}^{\omega_1}, \hat{\kappa}^{\omega_2}]] | 0 \rangle \end{aligned} \quad (3.38)$$

where \hat{P}_{12} has been defined in Equation 3.32. The second-order KS Hamiltonian $\hat{H}^{\omega_1, \omega_2}$ can be separated into two terms

$$\hat{H}^{\omega_1, \omega_2} = {}^1\hat{H}^{\omega_1, \omega_2} + {}^2\hat{H}^{\omega_1, \omega_2} \quad (3.39)$$

where ${}^1\hat{H}^{\omega_1, \omega_2}$ depends only on the first-order parameters $\hat{\kappa}^{\omega_1}$ and $\hat{\kappa}^{\omega_2}$, and ${}^2\hat{H}^{\omega_1, \omega_2}$ depends only on the second-order parameters $\hat{\kappa}^{\omega_1, \omega_2}$. Equation 3.38 can then be written

$$\begin{aligned} & \langle 0 | [\hat{\mathbf{q}}, [\hat{H}^{(0)}, \hat{\kappa}^{\omega_1, \omega_2}] - {}^2\hat{H}^{\omega_1, \omega_2}] | 0 \rangle - (\omega_1 + \omega_2) \langle 0 | [\hat{\mathbf{q}}, \hat{\kappa}^{\omega_1, \omega_2}] | 0 \rangle = \\ & \hat{P}_{12} \langle 0 | [\hat{\mathbf{q}}, [\hat{\kappa}^{\omega_1}, [\hat{\kappa}^{\omega_2}, \hat{H}^{(0)}]] + 2[\hat{\kappa}^{\omega_1}, \hat{V}^{\omega_2} + \hat{H}^{\omega_2}] + \omega_2[\hat{\kappa}^{\omega_1}, \hat{\kappa}^{\omega_2}] + {}^1\hat{H}^{\omega_1, \omega_2}] | 0 \rangle \end{aligned} \quad (3.40)$$

where all the second-order parameters now are on the left-hand side.

To solve the quadratic response functions (Eq. 3.31), the first-order parameters $\hat{\kappa}^{\omega_1}$ and $\hat{\kappa}^{\omega_2}$ are found by solving Equation 3.37. Then the $\hat{\kappa}^{\omega_1, \omega_2}$ parameter is found by solving Equation 3.40. In practice, these parameters are found by using a so-called trial vector (response vector) consisting of all the κ_{pq} in Equation 3.13.

3.3 PE contributions to the response functions

So far, the solvent effects through a polarizable embedding has been kept out of the discussion. The contributions from the polarizable embedding methods, that is both the explicit (QM/MM) and implicit (IEF-PCM) methods, do not enter the response functions (Eqs. 3.30 and 3.31) directly, but as an extra term in the n th-order Kohn-Sham Hamiltonian (Eq. 3.36)

$$\hat{H}^{(n)} = \sum_{pq} \left(\delta_{0n} h_{pq} + j_{pq}^{(n)} + v_{XC,pq}^{(n)} + v_{PE,pq}^{(n)} \right) \hat{E}_{pq} \quad (3.41)$$

where $v_{PE,pq}^{(n)}$ is the PE contribution to the n th-order expansion term of the time-dependent KS Hamiltonian. When working with linear and quadratic response theory we are only interested in the zeroth-, first- and second-order terms. That is $v_{PE,pq}^{(0)}$, $v_{PE,pq}^{(1)}$ and $v_{PE,pq}^{(2)}$. In the frequency domain, these contributions are given as $v_{PE,pq}^{(0)}$, $v_{PE,pq}^{\omega}$ and $v_{PE,pq}^{\omega_1,\omega_2}$. The zeroth-order contribution $v_{PE,pq}^{(0)}$ is, obviously, identical to the PE contribution to the time-independent KS Hamiltonian (Eq. 2.1 on page 17).

3.3.1 QM/MM response contributions

In the case of the explicit model developed by Kongsted and co-workers^{69,70}, the first-order (Eq. 3.42) and second-order (Eq. 3.43) terms from the PE, contributing to the first- and second-order KS Hamiltonian, are given as

$$v_{PE}^{\omega_i} = - \sum_{s=1}^S \mu_s^{\text{ind}}(\tilde{\mathbf{F}}^{\omega_i}) \hat{\mathbf{F}}_{s,\text{el}}^{(1)} \quad (3.42)$$

$$v_{PE}^{\omega_1,\omega_2} = - \sum_{s=1}^S \mu_s^{\text{ind}}(\tilde{\mathbf{F}}^{\omega_1,\omega_2}) \hat{\mathbf{F}}_{s,\text{el}}^{(1)} \quad (3.43)$$

⁶⁹J. M. Olsen, K. Aidas, and J Kongsted, *J. Chem. Theory Comput.*, 2010, **6**, 3721–3734.

⁷⁰J. M. H. Olsen and J. Kongsted, *Adv. Quantum Chem.*, 2011, **61**, 107–143.

where the induced dipoles are induced by the electric field from the perturbed densities. The operator $\hat{\mathbf{F}}_{s,\text{el}}^{(1)}$, where the superscript (1) is not related to the first-order transformation but to the interaction tensor (Eq. 2.15 on page 22), is defined as

$$\hat{\mathbf{F}}_{s,\text{el}}^{(1)} = - \sum_{pq} \int \rho_{pq}(\mathbf{r}) T_s^{(1)}(\mathbf{r}) d\mathbf{r} \hat{E}_{pq} \quad (3.44)$$

where $T_s^{(1)}(\mathbf{r})$ is the rank 1 interaction tensor⁵⁵.

The second-order term (Eq. 3.43) can be divided into two terms, one depending only on first-order terms and one depending on second-order terms, as for the KS Hamiltonian (Eq. 3.39)

$$\begin{aligned} v_{\text{PE}}^{\omega_1, \omega_2} &= {}^1v_{\text{PE}}^{\omega_1, \omega_2} + {}^2v_{\text{PE}}^{\omega_1, \omega_2} \\ &= - \sum_{s=1}^S \boldsymbol{\mu}_s^{\text{ind}}({}^1\tilde{\mathbf{F}}^{\omega_1, \omega_2}) \hat{\mathbf{F}}_{s,\text{el}}^{(1)} - \sum_{s=1}^S \boldsymbol{\mu}_s^{\text{ind}}({}^2\tilde{\mathbf{F}}^{\omega_1, \omega_2}) \hat{\mathbf{F}}_{s,\text{el}}^{(1)} \end{aligned} \quad (3.45)$$

The induced dipole moments entering Equations 3.42 and 3.45 are calculated using the transformed electric fields, given as

$$\tilde{\mathbf{F}}^{\omega_i} = \langle 0 | [\hat{\kappa}^{\omega_i}, \hat{\mathbf{F}}_{s,\text{el}}^{(1)}] | 0 \rangle \quad (3.46)$$

$${}^1\tilde{\mathbf{F}}^{\omega_1, \omega_2} = \langle 0 | [\hat{\kappa}^{\omega_1}, [\hat{\kappa}^{\omega_2}, \hat{\mathbf{F}}_{s,\text{el}}^{(1)}]] | 0 \rangle \quad (3.47)$$

$${}^2\tilde{\mathbf{F}}^{\omega_1, \omega_2} = \langle 0 | [\hat{\kappa}^{\omega_1, \omega_2}, \hat{\mathbf{F}}_{s,\text{el}}^{(1)}] | 0 \rangle \quad (3.48)$$

The polarizable QM/MM method is fully self-consistent at the response level, as it was for the ground-state energy. On the one hand, QM/MM contributes to the first- and second-order KS Hamiltonian, so it has an effect on the perturbed electronic density. On the other hand, the QM/MM contributions are polarized by the perturbed electronic density.

3.3.2 PCM response contributions

The derivation of the contribution to the response equations due to PCM is equivalent to QM/MM. In the nonequilibrium solvation regime, the apparent

charges due to the electronic density is divided into a dynamic and an inertial component⁷¹

$$\mathbf{q}_i = \mathbf{q}^N + \mathbf{q}_i^e \quad (3.49)$$

$$\mathbf{q}_d = \mathbf{q}_d^e \quad (3.50)$$

where only the dynamic ASC are taken into account when calculating the n th-order ASC. The reason for dividing the apparent charges into a dynamic (fast) and inertial (slow) part is that only the electrons in the solvent will move fast enough to react on the perturbed density of the solute⁷². The nuclei of the solvent will still be oriented as if the solute was in its ground-state. The way the separation is done is by using a matrix \mathbf{K}_d that is depending on the optical dielectric constant of the solvent (ϵ_∞), instead of the static dielectric constant (ϵ_0) that the matrix \mathbf{K} was depending on in Equation 2.9 (on page 20). The inertial component is then defined as the difference between the original and the dynamic one

$$\mathbf{q}_i = \mathbf{q}^N + \mathbf{q}^e - \mathbf{q}_d \quad (3.51)$$

The first- and second-order terms are then given as

$$v_{\text{PE},pq}^{\omega_i} = \mathbf{V}^{\omega_i} \cdot (\mathbf{q}^e + \mathbf{q}^N) + (\mathbf{V}^e + \mathbf{V}^N) \cdot \mathbf{q}_d^{\omega_i} \quad (3.52)$$

$$v_{\text{PE},pq}^{\omega_1,\omega_2} = \mathbf{V}^{\omega_1,\omega_2} \cdot (\mathbf{q}^e + \mathbf{q}^N) + \hat{P}_{12} \mathbf{V}^{\omega_1} \cdot \mathbf{q}_d^{\omega_2} + (\mathbf{V}^e + \mathbf{V}^N) \cdot \mathbf{q}_d^{\omega_1,\omega_2} \quad (3.53)$$

where \mathbf{V}^{ω_i} and $\mathbf{q}_d^{\omega_i}$ are the potentials and apparent surface charges on the tesseraes due to the first-order perturbed electronic density, and $\mathbf{V}^{\omega_1,\omega_2}$ and $\mathbf{q}_d^{\omega_1,\omega_2}$ are related to the second-order perturbed electronic density.

As for the polarizable QM/MM method, the PCM method is fully self-consistent in the response theory. Since PCM contributes to the n th-order

⁷¹L. Frediani, H. Agren, L. Ferrighi, and K. Ruud, *J. Chem. Phys.*, 2005, **123**, 144117.

⁷²This separation is automatically taken care of in the polarizable QM/MM method, where the static multipoles corresponds to the inertial components while the dynamical components is represented by the polarizabilities.

KS Hamiltonian, the PCM will affect the perturbed density. At the same time, the PCM response operators depend on the same perturbed electronic density.

Chapter 4

Summary of the papers

A short introduction to the papers included in this thesis will be presented in this chapter. The papers are listed on page VII. In Section 4.1 the three layered QM/MM/PCM model from Paper I is presented, while the parallelization of the QM/MM module in Dalton (Paper II) is presented in Section 4.2. In the last section of this chapter (Sec. 4.3), studies of one- and two-photon absorption properties in fluorescent proteins (Papers III, IV and V) are presented.

4.1 The three-layered QM/MM/PCM model

In Paper I, the implementation and theory of a fully polarizable three layered quantum mechanics/molecular mechanics/polarizable continuum model up to linear response was presented⁷³. The short-range interactions between the solute and the solvent were treated explicitly with polarizable classical mechanics (MM), while the long-range interactions were treated implicitly by means of a polarizable dielectric continuum model (PCM).

⁷³A. H. Steindal, K. Ruud, L. Frediani, K. Aidas, and J. Kongsted, *J. Phys. Chem. B*, 2011, **115**, 3027–3037.

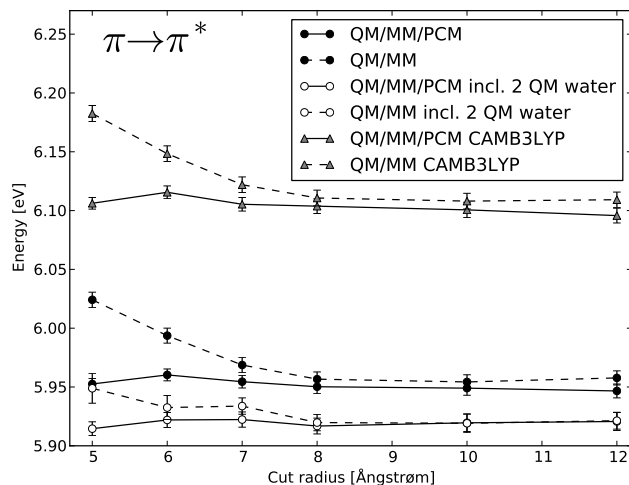


Figure 4.1: The dependence of cutoff radii on the excitation energies (eV) in acrolein surrounded by water molecules, as reported in Paper I

This was the first implementation⁷⁴ where the interaction between polarizable MM and PCM was included at the response level. Previously, the interactions were only present when computing the energy, while the interaction between MM and PCM was not included when solving the response equations⁷⁵. In practice, the coupling between MM and PCM was obtained by deriving the apparent surface charges and potentials on the cavity in PCM in the presence of the static multipoles and induced dipoles from the MM region (see equations 2.8 on page 20). At the same time, the induced dipoles in the MM module were calculated in the presence of the electric field due to the ASC. Thus, the MM and PCM are coupled and the calculations have to be done self-consistently. The coupling between MM and PCM is done in an equivalent way when calculating linear response properties: the induced

⁷⁴But not the last. See for instance S. Caprasecca, C. Curutchet, and B. Mennucci, *J. Chem. Theory Comput.*, 2012, **8**, 4462-4473 and F. Lipparini, C. Cappelli, G. Scalmani, N. De Mitri, and V. Barone, *J. Chem. Theory Comput.*, 2012, **8**, 4270-4278.

⁷⁵See for instance H. Li, *J. Chem. Phys.*, 2009, **131**, 184103.

dipoles due to the perturbed electric field is taken into account when calculating the ASC, while these ASCs are taken into account when calculating the induced dipoles.

Our implementation was tested by studying the one-photon vertical excitations in three molecules in aqueous solution, namely acetone, acrolein and pyridine. A faster convergence with respect to system size was found for QM/MM/PCM compared to QM/MM (see for instance Figure 4.1). In other words, the amount of explicit water molecules needed in the calculations were dramatically reduced.

4.2 Parallelization of the QM/MM module

In Paper II the parallelization of the PE-DFT module in the Dalton program was described, as well as demonstration of the scaling efficiency. The parallelization was performed for all parts of the code where one-electron integrals had to be computed, that is calculating the contribution to the KS Hamiltonian (Eq. 2.10), as well as the PE contribution to the n th-order KS Hamiltonian (Eq. 3.41) up to third-order (cubic response).

The so-called master-slave approach was used, where one of the computing cores is distributing tasks to all the other cores. The master core is told when a slave core is free to do another task. In that way a good load balance was achieved. A satisfactory gain factor was obtained up to 1000 cores⁷⁶, as shown in Figure 4.2 One reason why the master-slave approach was beneficial for the QM/MM module was that the calculations consisted of a large number of independent tasks, namely calculations for every classical site.

The parallelization of the QM/MM module in Dalton was absolutely necessary for us in order to do calculations on the fluorescent proteins as investi-

⁷⁶A. H. Steindal, J. M. H. Olsen, L. Frediani, J. Kongsted, and K. Ruud, *Mol. Phys.*, 2012, **110**, 2579–2586.

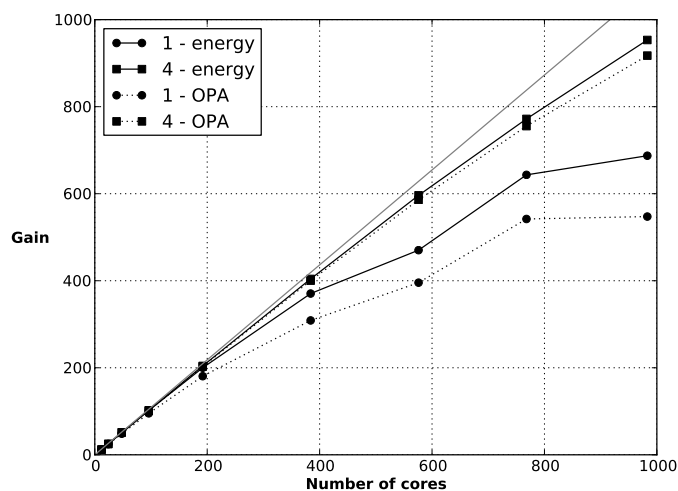


Figure 4.2: Scaling of the QM/MM module in the DALTON code, as given in Paper II.

gated in Papers III, IV and V.

4.3 Polarizable embedding on fluorescent proteins

The parallelized QM/MM module was used to calculate the one-photon and two-photon absorption properties in the green fluorescence protein (GFP)⁷⁷. This work is presented in Paper III. The crystal structure with the pdb-code 1EMB was used, and the polarizable embedding where the protein was represented by an advanced force-field consisting of higher-order multipoles and anisotropic polarizabilities located on every atom.

The importance of polarization was demonstrated, as well as the importance

⁷⁷A. H. Steindal, J. M. H. Olsen, K. Ruud, L. Frediani, and J. Kongsted, *Phys. Chem. Chem. Phys.*, 2012, **14**, 5440–5451.

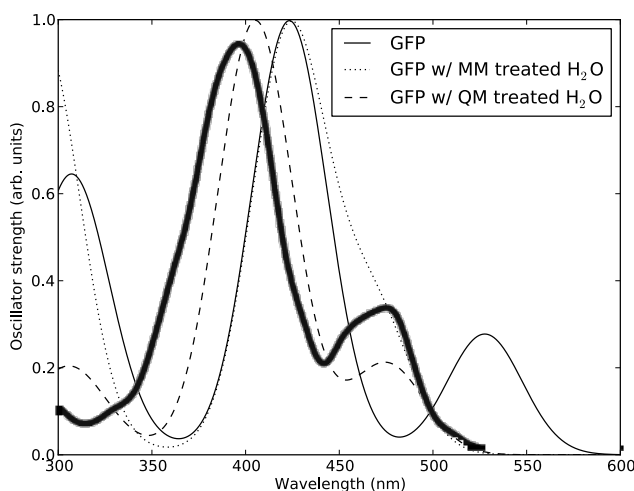


Figure 4.3: The full calculated absorption spectrum of GFP, as reported in Paper III.

of including crystal water surrounding the chromophore. The latter had to be described by quantum mechanics when the neutral chromophore was investigated in order to reproduce experimental data (see Figure 4.3). A comparison between classical and quantum mechanical description of amino acid in vicinity of the chromophore was also conducted, and the classical description was found to be on par with the quantum mechanical description.

We went a step further in Paper IV, calculating OPA in a selection of different fluorescent proteins by the use of PE-DFT. Several approaches were investigated, including the use of the crystal structure directly, as done in Paper III, the use of molecular dynamics calculations, and optimizing the structures with QM/MM while keeping the protein fixed. Contrary to the previous article, we were not able to reproduce the experimental observed excitation energies. On the other hand, we demonstrated the importance of optimizing the chromophore of the crystal structures prior to the excitation energies calculations. Both the difference in excitation energies between different protein mutants, as well as the bathochromic shift in excitation energies be-

tween vacuum and protein for wtGFP were reproduced (see Figure 4.4). The

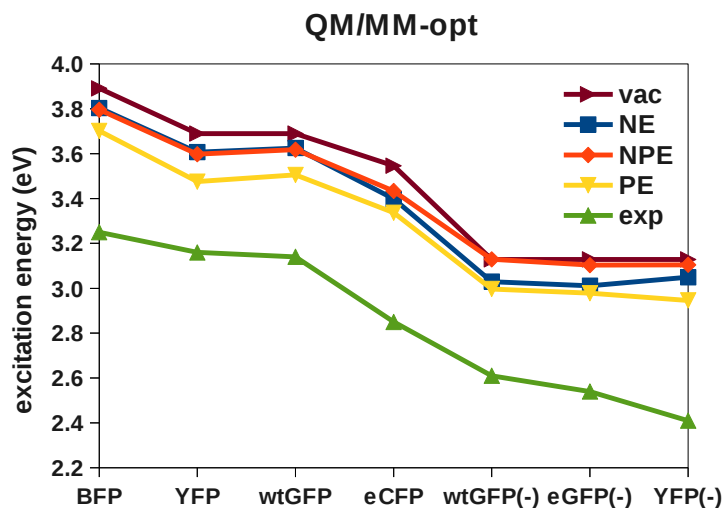


Figure 4.4: The excitation energies in fluorescent proteins calculated with different models (no embedding, non-polarizable embedding and polarizable embedding), as reported in Paper IV

bathochromic shifts, especially for the anionic wtGFP chromophore, were more pronounced for the polarizable embedding (PE) compared to no embedding (NE) and non-polarizable embedding (NPE).

In Paper V the importance of the surrounding protein on the two-photon absorption intensities in DsRed, a fluorescent protein, was investigated⁷⁸. Our calculations demonstrated an increase in TPA cross section, as well as a blue-shift in the excitation energy, in the DsRed chromophore when it was inside the protein, compared to the chromophore in vacuum. These changes were both because of structural changes of the chromophore and because of interaction between the chromophore and the surrounding protein. The

⁷⁸N. H. List, J. M. H. Olsen, H. J. A. Jensen, A. H. Steindal, and J. Kongsted, *J. Phys. Chem. Lett.*, 2012, **3**, 3513–3521.

increase in TPA cross section was found to originate from an increased change in the permanent dipole moment between the ground and excited states. Further, we demonstrate the importance of certain amino acids on the optical properties of the DsRed protein.

Paper 1

Paper 2

Paper 3

Paper 4

Paper 5

